Antireflection Microstructured Surface on ZnSe for Mid-infrared Spectral Region

Jia-Ji Cao, Qian-Kun Li, Yan-Hao Yu, and Yong-Sen Yu*

State Key Laboratory on Integrated Optoelectronics, College of Electronic Science and Engineering, Jilin University, Changchun 130012, Peoples Republic of China
**E-mail: yuys@jlu.edu.cn*

Antireflection microstructured surface were fabricated on ZnSe through a rapid and scalable method which was called femtosecond laser direct writing (FsLDW). With this technology, micrometer level inverted pyramid and cone arrays were fabricated precisely. The measured transmittance were about 11.3% higher compared with the plain ZnSe at 9μm in the ideal situation. These results were in good accord with the simulations which were calculated by geometric and diffractive field tracing techniques.
DOI: 10.2961/jlmn.2019.02.0001
Keywords: antireflection, subwavelength structure, diffractive optics, ZnSe, femtosecond laser direct writing

1. Introduction

Zinc selenide (ZnSe) is an ideal and promising material for applications to the infrared band optical and electronic devices [1–4], such as window in solar battery, fairing and convex lens. This kind of material also used as laser crystal of mid-infrared solid-state laser [5], which become a hot topic in domestic and overseas research for its widespread application value and prospect in remote sensing of atmosphere, laser radar, spectroscopy, national defense and spaceflight aviation. The refractive index of ZnSe from 2 μm to 15 μm is about 2.4, which caused high surface reflectance [6, 7]. In the traditional way, single- or multilayer film coating technology is used to manipulate the high and low refractive indices [8–10]. However, multiple problem may arise after the film coating [11–13]. First, the optical properties of the coating may be damaged by dust, defects, humidity or other kinds of environmental degradations. Second, the refractive index of the coating material may not match with bulk material. Most of all, the coating may cracking or shedding when the outside temperature changed dramatically, which is unsuitable for high power laser or spacecraft. Antireflection microstructured surface prepared on the material can easily overcome these problems. Compared with film coating, antireflection microstructured surface can be equivalent to a gradient film system with refractive index range from air to material [14].

After first discovered by Bernard in 1968, researchers have conducted a detailed study of antireflection microstructured surfaces [15]. This opened the way for those who did this research later. In the early nineties, with holographic approach, antireflective sub micrometer surface-relief gratings were produced on various stand positive photoresists with an area of 190 mm×166 mm [16]. Which can produce large-area antireflection microstructures efficiently. However only quasi-sinusoidal structures can be produced with this kind of method, as well as the structure may breaks if it is way too deep. Joachim P. Spatz fabricated highly light transmissive interfaces for antireflective optics in the deep-UV range which were prepared by nanolithography and reactive ion etching [17]. With this kind of fabrication method, plan convex fused silica lenses were demonstrated with an increased transmittance of light between 185 and 300 nm. Which were of great use in deep-UV range. Whereas the experimental procedure was quite complex. Block copolymer self-assembly and plasma etching were also leveraged to fabricate enhanced broadband antireflection in silicon solar cells. Though the hydrogen bromide and chlorine used during inductively coupled plasma-reactive ion etching were not environmentally friendly. To overcome these problems, femtosecond laser direct writing (FsLDW) has the superiority in high peak power and the accuracy in three-dimensional machining which have been used in micro-nano fabrication [18–26].

In this letter, we fabricated antireflection microstructure on ZnSe for mid-infrared spectral range with femtosecond laser direct writing (FsLDW) technology. High accuracy inverted pyramid and cone arrays with different arrangement mode were fabricated on ZnSe. This device is much more stable because antireflection microstructure and ZnSe are integrated. Which may have potential applications in infrared detection and imaging technology.

2. Materials and Methods

The mathematical models currently used for describing the propagation characteristics of electromagnetic fields mainly include effective medium theory (EMT), finite-difference time-domain method (FDTD), finite element method (FEM) and rigorous coupled wave method (RCWA). Because of the period of the antireflection microstructure is much smaller than the incident wavelength, effective medium theory (EMT) were chose to do the analysis. This theory explains that when an electromagnetic wave propagated through a grating which is much smaller than it, there would be only one reflection and one transmission wave in the zero order grating. The following grat-

ing equation determines whether a diffraction order could propagates or not,

$$n_s \sin\theta_m = \frac{m\lambda}{\Lambda} + n_i \sin\theta_i \quad (1)$$

n_i represents the refraction index when the light incidentting to the medium, n indicates the refraction index when the light transmitting through the medium (when it come to the reflection diffraction orders, $n=n_i$. As for the transmission diffraction, n would be the same as the substrate's refraction index.) Using θ_m and θ_i to represent the angle of the m order and the angle of incident wave which are measured from the grating's surface normal, respectively. λ is on behalf of the wavelength of the incident free space, and Λ is the grating period. When the high order diffraction fields are forced to be evanescent, a zero order grating is produced. The inequality of the periodic of 2D grating and wavelength would be determined by

$$\frac{\Lambda_x}{\lambda} < \frac{1}{[\max(n_s^2, n_i^2) - (n_i \sin\theta_i \sin\phi_i)^2]^{1/2} + |n_i \sin\theta_i \cos\phi_i|} \quad (2)$$

$$\frac{\Lambda_y}{\lambda} < \frac{1}{[\max(n_s^2, n_i^2) - (n_i \sin\theta_i \sin\phi_i)^2]^{1/2} + |n_i \sin\theta_i \cos\phi_i|} \quad (3)$$

Max were used to refer the maximum value of either n_s or n_i. The period of the grating divided by the wavelength of operation ($\Lambda\lambda$) can be used to define the normalized grating period. When the grating is designed at all incidence for the experiment, the normalized period of the grating reduces to,

$$\Lambda < \frac{\lambda}{\max(n_s, n_i) + n_i} \quad (4)$$

The refractive index of ZnSe from 2 to 15 μm is about 2.4, so 2.4 was brought into inequality above. We choose 9 μm as the incident wavelength, then we got the period of the grating, Λ=2.9 μm. In order to calculated the value of the minimum depth of the structured, following formula were used,

$$d_{\min} = \frac{\lambda}{4\sqrt{n_s n_i}} \quad (5)$$

In this way, the minimum depth of antireflection microstructure is about 1.45 μm. Processing capability was proved in the structure we prepared in Figure 1. The fluence of the laser were 0.13 mJ/cm^2, 0.2 mJ/cm^2, 0.48 mJ/cm^2, 0.87 mJ/cm^2 respectively. It could be seen that the width of the structures were getting wider as the laser power increasing. The depth of the structures were getting deeper as the laser power increasing. The experiment of processing effects at different fluence facilitates the later fabricating of antireflection microstructures. Therefore, required antireflection microstructure can be prepared easily by adjusting the laser power.

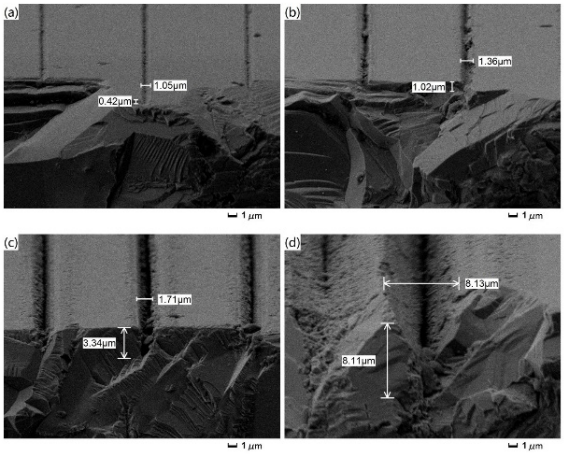

Fig.1 Dependence of width and depth of the line structures on laser power. (a) 0.13 mJ/cm^2; (b) 0.2 mJ/cm^2; (c) 0.48 mJ/cm^2 and (d) 0.87 mJ/cm^2.

Figure 2 shows the optical path of the experiment. Antireflection microstructured surfaces were fabricated by a commercial Ti:Sapphire laser (Spectra-Physics), with the ability to deliver 120 fs pulses at 2.5 kHz repetition rate at a 800 nm center wavelength. The ablation fluence of the laser was 0.174 mJ/cm^2 during the experiment. Due to the diffraction limit of the interaction between the laser and the material, BBO crystal were used to double the frequency. With an 80× objective lens, collimated beam was focused on a piece of ZnSe. To reach the repeatability and accuracy of each experiment, a variable neutral-density filter were inserted between the laser and the lens. We used a nanometer precision piezo stage (PI P-622 ZCD) and a galvano mirror to control the movement of the material and the laser beam. 3D geometry of various microstructure were firstly designed by the C programming language, and used it for our manufacturing. The sample is attached to the piezo stage by water. And the top surface of it can be seen clearly by a silicon charge-coupled device (CCD) (HD-GY500), with a spectral response range from 400nm to 1000nm. After trying different fabricating parameters, we fixed single pulse exposure time at 1000μs and the scanning interval is 100nm. Acetone, alcohol and deionized water were used before and after the fabrication to remove the dust and the debris.

3. Results

Four different arrangements of antireflection microstructure were obtained by a scanning electron microscope (SEM) which were showed in Figure 3. Pyramid-square, pyramid-hexagon, cone-square and cone-hexagon arrangements of antireflection microstructure were fabricated with

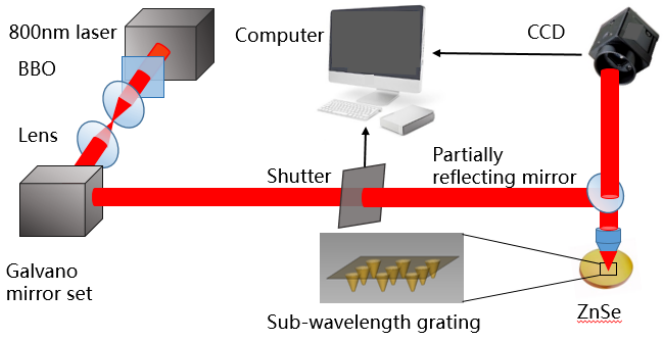

Fig.2 This is an illustration of the femtosecond laser fabricating anti-reflection microstructured surface on the ZnSe.

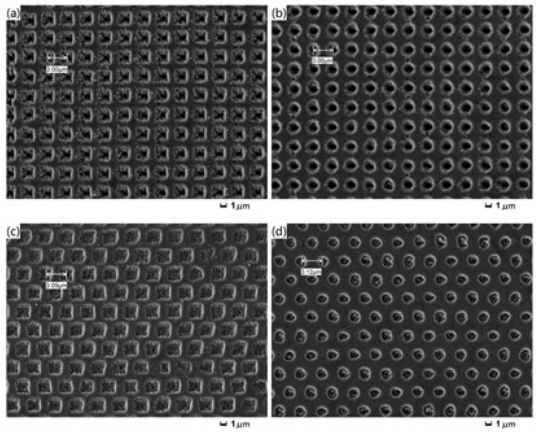

Fig.3 The SEM image of the sub-wavelength antireflection microstructure. (a) Pyramid-square; (b) Pyramid-hexagon; (c) Cone-square and (d) Cone-hexagon.

different designs. The electrical conductivity of the sample were improved by an Au film. This 10 nm film was sputtered with an auto fine coater (JFC-1600; JEOL) at a current of 20 mA for 60 s before the SEM. The subwavelength microstructures had a period of 3 μm and a depth of 2 μm which were of good surface morphology. Pyramid and square structure can cause a slightly different in transmission spectrum. Fabricating time can be reduced by a wide margin with the inverted structure we design. Which is 5 minutes during the experiment. In order to improve the femtosecond laser direct writing efficiency, field lens with the focal length of 10cm can also be used during the fabrication. With this kind of fabricating equipment, 1 cm×1 cm antireflection microstructure can be produced within 20 minutes at the same situation.

Highly magnified laser scanning confocal microscopy (LSCM) were also used to reveal the three dimensional profile of the antireflection microstructure. The depth and the width of pyramid-square, pyramid-hexagon, cone-square and cone-hexagon arrangements of antireflection microstructure were shown in Figure 4. The horizontal and vertical profile information of the antireflection

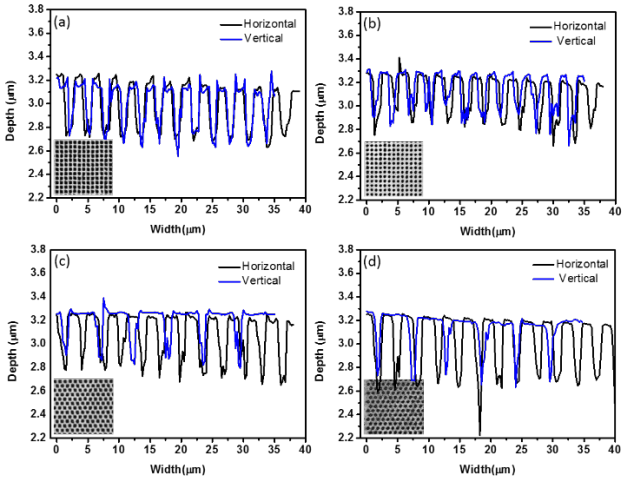

Fig.4 The LSCM image and the profile information of the sub-wavelength antireflection microstructure. (a) Pyramid-square; (b) Pyramid-hexagon; (c) Cone-square and (d) Cone-hexagon.

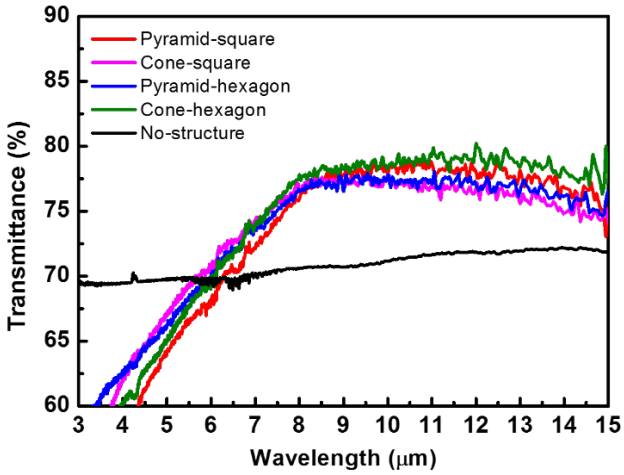

Fig.5 Measured transmittance of fabricated sub-wavelength antireflection microstructure on the ZnSe using Fourier transform infrared spectrometer.

microstructure were given in black and blue line.It can be seen from the figure that the sturcture is uniform and consistent with the design.

The transmittance of the pure ZnSe and the structures were carried out with a Fourier transform infrared spectrometer (FT-IR, Nicolet 6700), which were based on the principle of Fourier transform. With the help of the Origin 9.0, the transmittance of different structures were shown in Figure 5. The transmittance of the pure ZnSe is only about 70%. With antireflection microstructure, the transmittance were improved from 6μm to 15μm. Solid lines of different colors represents different arrangements of antireflection microstructure. The red, pink, blue, green line represent pyramid-square, cone-square, pyramid-hexagon and cone-hexagon arrangement of the antireflection microstructure respectively. It has been shown from the green line that the cone-hexagon structure has a slightly higher transmittance, which were about 80%. Figure 6 is the simulation of the inverted cone-square structure calculated by Virtual Lab. In the simulation, the wavelength range of the incident light were set from 12 μm to 15 μm.

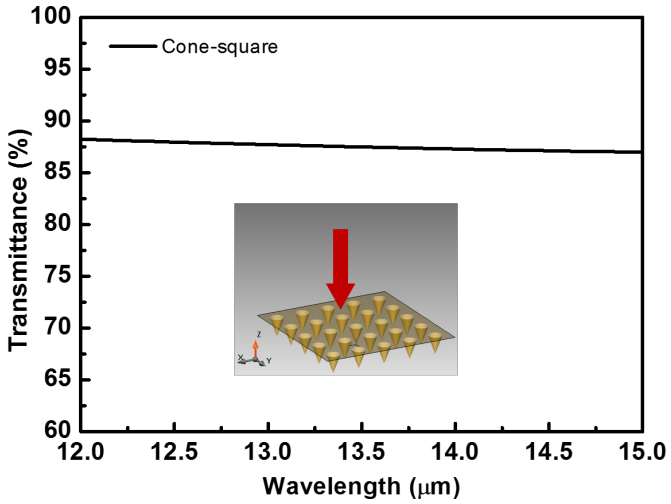

Fig.6 Simulation result of the inverted cone-square transmittance performance.

The transmittance of the cone-square were about 87%. It could be seen that the experiment result were in good accord with the simulation.

4. Conclusions

In conclusion, micron scale antireflection microstructured surface can be manufactured by femtosecond laser direct writing technology on hard material. With this kind of processing method, the transmittance of the sample can be improved economically and quickly. Different arrangements of antireflection microstructure have slightly different antireflection effect. The transmittance of ZnSe were improved from 70% to about 80% in the Mid-infrared region. In order to further improve the transmittance of the sample, both side structure can be prepared. This kind of structures may have a good application prospects in Mid-infrared imaging and measurement.

Acknowledgments

This work was supported by National Key R&D Program of China (2017YFB1104600) and National Nature Science Foundation of China (NSFC) (61590930, 21473076, 61605055 and 61435005).

References

[1] J. Kvietkova, B. Daniel and M. Hetterich: Thin Solid Films, 455, (2004) 228.
[2] M. A. Abdel-Rahim, M. M. Hafiz and A. E. B. Alwany: Opt. Laser Technol., 47, (2013) 88.
[3] N. Zeiri, A. B. Nasrallah, N. Sfina and M. Said: Infrared Phys. Techn., 64, (2014) 33.
[4] Y. Qu, Z. H. Kang, T. J. Wang, Y. G. Jiang, Yu. M.Andreev and J. Y. Gao: Laser Phys. Lett., 4, (2010) 238.
[5] P. Kannappan, K. Baskar, J. B. M. Krishna, K. Asokan, C. L. Dong and C. L. Chen: Mater. Sci. Semicon. Proc., 36, (2015) 140.
[6] D. C. Harris: Infrared Phys. Technol., 39, (1998) 185.
[7] H. H. Li: Journal of Physical and Chemical Reference Data, 13, (1984) 103.
[8] M. Shokooh-Saremi and M. M. Mirsalehi: Appl. Opt., 44, (2005) 3877.
[9] A. L. Pénard, T. Gacoin and J. P. Boilot: Acc. Chem. Res., 38, (2007) 895.
[10] L. Martinu and D. Poitras: J. Vac. Sci. Technol. A, 18, (2000) 2619.
[11] H. K. Raut, V. A. Ganesh and A. S. Nair: Energy Environ. Sci., 4, (2011) 3779.
[12] S. P. Min, Lee. A. Youngmin and K. K Jim: Chem. Mater.,17, (2005)
[13] J. Amirloo, S. S. Saini and M. Dagenais, J. Vac. Sci. Technol. A, 34, (2016) 061505.
[14] Y. Ono, Y. Kimura, Y. Ohta and N. Nishida: Appl. Opt., 26, (1987) 1142.
[15] W. H. Miller, G. D. Bernard, J. L. Allen: Science, 162, (1968) 760.
[16] A. Gombert, K. Rose, A. Heinzel A, W. Horbelt, C. Manecke, B. Bläsi and V. Wittwer: Sol. Energy Mater. Sol. Cells, 54, (1998) 333.
[17] T. Lohmüller, M. Helgert, M. Sundermann, R. Brunner and J. P. Spatz: Nano Lett., 8, (2008) 1429.
[18] G. Q. Du, Q. Yang, F. Chen, H. W. Liu, Z. F. Deng, H. Bian, S. G. He, J. H. Si, X. W. Meng and X. Hou: Opt. Lett., 37. (2012) 4404.
[19] L. Wang, Q. D. Chen, X. W. Cao, R. Buividas, X. Wang, X. W. Wang, S. Juodkazis and H. B. Sun: Light Sci. Appl., 6, (2017), e17112.
[20] R. Kammel, R. Ackermann, J. Thomas, J, Götte, S. Skupin, A. Tu¨nnermann and S. Nolte: Light Sci. Appl., 3, (2014) e169.
[21] H. Imamoto, S. Kanehira, X. Wang, K. Kametani, M. Sakakura, Y. Shimotsuma, K. Miura, and K. Hirao: Opt. Lett., 36, (2011) 1176.
[22] S. Juodkazis, K. Nishimura, H. Misawa, T. Ebisui, R. Waki, S. Matsuo and T. Okada: Adv. Mater., 18, (2006) 1361.
[23] K. Sugioka, Y. Cheng: Light Sci. Appl., 3, (2014) e149.
[24] X. Q. Liu, Q. D. Chen, K. M. Guan, Z. C. Ma, Y. H. Yu, Q. K. Li, Z. N. Tian and H. B. Sun: Laser Photon. Rev., 11, (2017) 1600115.
[25] H. Wang, Y. L. Zhang, W. Wang, H. Ding and H. B. Sun: Laser Photon. Rev., 11, (2017) 1600116.
[26] L. Jiang, A. D Wang, B. Li, T. H. Cui and Y. F. Lu: Light Sci. Appl., 7, (2018) 17134.

(Received: June 27, 2018, Accepted: April 2, 2019)